Article

Discovery Medicine 2026; 38(206): 789–801
https://doi.org/10.24976/Discov.Med.202638206.65

Pterostilbene Intervenes in Neuroinflammation and Abnormal Phosphorylation of Tau Protein in Alzheimer's Disease by Inhibiting Bace 1

Linying Li[1,2], Haitao Li[2], Mantong Zuo[2], Xiaomin Wang[1]*

[1]Department of Neurobiology, School of Basic Medical Sciences, Capital Medical University, 100069 Beijing, China
[2]Yanjing Medical College, Capital Medical University, 101300 Beijing, China
*Correspondence: xmwang@ccmu.edu.cn (Xiaomin Wang)
Submitted: 27 November 2025 Revised: 23 January 2026 Accepted: 26 February 2026 Published: 20 March 2026

Background: Alzheimer's disease (AD) is characterized by neuroinflammation, amyloid-β (Aβ) accumulation, and abnormal microtubule-associated protein tau (Tau) phosphorylation. This study evaluates the therapeutic potential of pterostilbene (PTS), a natural compound with anti-inflammatory activity, in an Aβ1-42-induced AD mouse model.

Methods: AD mice were established by intraperitoneal injection of aggregated Aβ1-42 and were subsequently treated with PTS, donepezil, or PTS combined with a β-site amyloid precursor protein–cleaving enzyme 1 (BACE1) upregulating agent. Cognitive performance was assessed through behavioral tests, and AD-related pathology was evaluated using Enzyme-linked immunosorbent assay (ELISA), immunofluorescence, reverse transcription quantitative polymerase chain reaction (RT-qPCR), and Western blotting.

Results: Compared with AD mice, PTS treatment significantly improved cognitive performance in behavioral tests ($p < 0.01$), reduced hippocampal Aβ immunoreactive deposition and decreased soluble and insoluble Aβ40/42 levels ($p < 0.01$), and markedly inhibited Tau phosphorylation at Ser396 and Thr231 ($p < 0.01$). PTS also significantly suppressed neuroinflammatory responses, as evidenced by reduced levels of tumor necrosis factor-alpha (TNF-α), interleukin-1 beta (IL-1β), and interleukin-6 (IL-6), together with downregulation of microglia- and astrocyte-associated proteins ($p < 0.01$). At the molecular level, PTS was associated with reduced expression of BACE1, Clathrin, and Nicastrin as well as inhibition of the nuclear factor kappa B (NF-κB) pathway, as reflected by decreases in NF-κB p65 subunit (p65) and phosphorylated inhibitor of nuclear factor kappa B alpha (p-IκBα) levels, along with restoration of IκBα expression ($p < 0.01$). Co-treatment with the BACE1 upregulation–associated agent partially attenuated the protective effects of PTS.

Conclusion: PTS exerts significant neuroprotective effects in an Aβ1-42-induced AD mouse model by alleviating cognitive impairment, amyloidogenic pathology, neuroinflammation, and Tau hyperphosphorylation, potentially through modulation of BACE1-related processes and NF-κB signaling. PTS may represent a promising multi-target therapeutic candidate for AD.

Keywords: pterostilbene; Alzheimer's disease; neuroinflammation; Tau protein phosphorylation; NF-κB signaling pathway

Introduction

Alzheimer's disease (AD) represents a major neurodegenerative disorder characterized by progressive clinical deterioration, including memory impairment, cognitive decline, and behavioral abnormalities [1,2]. As the leading cause of dementia in older adults, AD has a profound impact on global public health. Dementia affects over 50 million people globally, as reported by the World Health Organization (WHO), with 60%–70% of cases attributable to AD [3]. By 2050, global estimates predict a rise in the number of individuals living with dementia to nearly 152 million, especially in regions with rapidly aging populations, such as Asia. In China, there are more than 10 million AD patients, and new cases continue to rise annually [4,5]. The high prevalence of this disease and the medical costs impose a substantial socioeconomic burden on patients' families and society at large. Accordingly, exploring the underlying pathogenesis of AD and developing safe and effective therapeutic strategies remain urgent priorities.

Currently, clinical therapeutic strategies for AD mainly include symptom-relieving drugs and pathology-specific treatments [6–8]. Among them, cholinesterase inhibitors (e.g., donepezil, galantamine) and N-methyl-D-aspartate (NMDA) receptor antagonists (e.g., memantine) can alleviate the deterioration of cognitive function, but have limited effects on pathological progression [9,10]. In recent years, immunotherapy strategies targeting the core pathological features of AD — amyloid-β (Aβ) plaque clearance and microtubule-associated protein tau (Tau) protein phosphorylation—have attracted considerable attention [11]. However, many clinical trials have shown limited

efficacy, and such approaches may be accompanied by serious adverse reactions, such as cerebral edema and hemorrhage [12,13]. The limitations of the above treatments have prompted increasing interest in multi-target, low-toxic natural active compounds, which have gradually become the focus of AD treatment research due to their multifaceted biological effects and favorable safety profiles.

Pterostilbene (PTS) is a naturally derived benzofuran compound that is mainly present in blueberries and Pterostilbene plants [14,15]. Its superior pharmacokinetic properties, such as strong lipid solubility and high bioavailability, give it significant advantages in the treatment of various diseases. Studies have shown that PTS has anti-inflammatory, antioxidant and neuroprotective effects, particularly in neurodegenerative diseases, suggesting its potential therapeutic value [16,17]. In the studies of AD, PTS can reduce neuroinflammation through the inhibition of the nuclear factor kappa B (NF-κB) axis, can enhance Aβ-degrading enzyme activity to reduce Aβ deposition, regulate Tau protein phosphorylation-related kinases to inhibit the neurofibrillary tangle formation, and alleviate oxidative stress damage to neurons [18,19]. Furthermore, BACE1 (β-site amyloid precursor protein-cleaving enzyme 1), a key protease responsible for Aβ generation, is increasingly recognized as a critical therapeutic target owing to its role in promoting Aβ accumulation, neuroinflammation, and abnormal Tau phosphorylation [20,21]. Although PTS has demonstrated efficacy in targeting Aβ and Tau pathology, its potential interaction with BACE1 and the resulting multifaceted therapeutic effects remain unclear.

Based on current evidence, this study utilized an Aβ1-42-triggered mouse model to investigate the impact of PTS on learning- and memory-related impairments associated with AD. A pharmacological intervention associated with BACE1 upregulation was applied to explore the involvement of BACE1-related signaling in PTS-mediated regulation of Aβ accumulation, neuroinflammatory responses, and Tau phosphorylation. Through integrated behavioral and molecular analyses, this study aimed to characterize the multi-target actions of PTS and to provide an experimental basis supporting its viability as a therapeutic approach for AD.

Materials and Methods

Modeling and Grouping

C57BL/6 mice (2–3 months old, from Beijing Vital River Laboratory Animal Technology Co., Ltd., SPF grade) were kept under controlled conditions (22 $\pm$ 2 °C, 50–60% relative humidity, 12-h light/dark cycle), and were provided ad libitum access to standard chow and water. An AD mouse model was established by intraperitoneal injection of Aβ1-42. The Aβ1-42 peptide (Sigma-Aldrich, St. Louis, MO, USA; A9810) was dissolved in sterile saline to a final concentration of 82 µmol/L and incubated at 37 °C for 48 hours prior to administration to promote peptide aggregation, following commonly used protocols in Aβ-induced mouse models [22,23]. Then, mice were intraperitoneally injected with 200 µL of Aβ1-42 solution, once per mouse, to induce AD-related pathological changes. Intraperitoneal administration of pre-incubated Aβ1-42 was employed to induce Aβ-associated neuroinflammatory responses and amyloidogenic alterations in the brain.

Mice were allocated at random into five groups (n = 10 per group). The control group (Control) was gavaged with saline (10 mL/kg) daily from the 8th week. The AD model group (AD) received an intraperitoneal injection of Aβ1-42 (82 µmol/L) to induce AD, followed by daily saline gavage (10 mL/kg) from the 8th week. The AD+PTS group was gavaged with pterostilbene (30 mg/kg; Sigma-Aldrich, St. Louis, MO, USA; P1499) daily from the 8th week, and the AD+positive control group (POS) was gavaged with donepezil (2.5 mg/kg; Sigma-Aldrich, St. Louis, MO, USA; D6821) daily. The AD+PTS+3-NP group received Aβ1-42 to induce AD, followed by pterostilbene administration (30 mg/kg, gavage) starting from the 8th week. To induce mitochondrial dysfunction and oxidative stress, mice in this group were intraperitoneally injected with 3-nitropropionic acid (3-NP, 30 mg/kg; Sigma-Aldrich, St. Louis, MO, USA; N5636) once daily for 7 consecutive days, as previously described [24]. Upon completion of the study, mice were sacrificed via gradual carbon dioxide (CO_2) inhalation using a controlled, non-prefilled exposure method, in compliance with the American Veterinary Medical Association (AVMA) recommendations for animal euthanasia, with death subsequently verified. Brain tissues were promptly harvested for downstream biochemical and histological assessment.

All animal experiments complied with the ethical requirements of the Experimental Animal Welfare Ethics Committee of Capital Medical University and were approved under protocol number AEEI-2020-139.

Animal Behavior Test

Spatial learning and memory assessment using the Morris water maze. Prior to testing, mice were acclimated to the laboratory environment for 24 h. The apparatus comprised a circular pool (120 cm diameter, 50 cm height) filled with water to a depth of 30 cm, kept at 22 $\pm$ 1 °C. A platform was submerged 1 cm beneath the water surface and consistently positioned in a fixed quadrant. All mice underwent four training trials per day over a 4-day acquisition phase, with each trial lasting up to 60 s. If a mouse failed to locate the platform within the allotted time, it was gently guided to the platform and allowed to remain there for 15 s. The mouse's escape latency (the time required to find the platform), the number of crossings over the intersection of the platform quadrant, and the time spent in the target quadrant were recorded. After the experiment, a spatial exploration test was conducted in which the platform was removed, and

the swimming time the mice spending in the target quadrant was recorded.

The novel object recognition test (NORT) was used to evaluate the recognition memory in mice. The procedure consisted of an adaptation phase and a testing phase. During adaptation, mice were given 10 min of free exploration within the experimental arena. In the testing phase, two identical objects (familiar objects, TF) were positioned in fixed locations in the arena, and the mice were permitted to explore for 5 min. Following a 24-h interval, one of the familiar objects was replaced with a novel object (TN), and mice were reintroduced to the arena for an additional 5 min. Exploration time directed toward each object was quantified, and the recognition index was calculated using the formula RI = TN / (TF + TN). Exploration was operationally defined as nose-oriented investigation within 1 cm of the object, including sniffing or visual inspection.

The Y-maze test was applied to assess working memory and exploratory activity in mice, utilizing an apparatus with three arms (40 cm length, 3 cm bottom width, 13 cm upper width, and 15 cm wall height; BrainScience Idea, Co., Ltd., Osaka, Japan; YM-40M). Mice were placed in the central zone, and their arm entries along with alternation behavior were monitored over a 10-min session using EthoVision XT (version 15.0, Noldus Information Technology, Wageningen, Netherlands). Working memory was quantified as the proportion of correct alternations relative to the total number of novel arm entries.

Enzyme-Linked Immunosorbent Assay (ELISA)

Inflammatory cytokines (tumor necrosis factor-alpha (TNF-α), interleukin-1 beta (IL-1β), and interleukin-6 (IL-6)) and Aβ40 and Aβ42 levels in brain tissue were quantified using ELISA. The ELISA kit (Beyotime Biotechnology Co., Ltd., Shanghai, China; P0205S) used in the experiment was operated strictly following the manufacturer's protocol. Samples and standards were loaded onto antibody-precoated plates, followed by incubation, washing, and enzymatic reaction, with absorbance (OD value) recorded at 450 nm. Target protein concentrations were determined from the standard curve. Each sample was measured in triplicate to ensure technical reliability. Both soluble and insoluble Aβ contents were adjusted according to total protein levels and reported as pg/mg protein.

Immunofluorescence

Brain tissue was fixed in 4% paraformaldehyde (Beyotime Biotechnology Co., Ltd., Shanghai, China; P0099) for 24 hours, dehydrated with sucrose gradient and embedded in optimal cutting temperature compound (OCT; Beyotime Biotechnology Co., Ltd., Shanghai, China; C0171A). Frozen sections were prepared at a thickness of 10 µm. The sections were treated with 0.3% Triton X-100 (Beyotime Biotechnology Co., Ltd., Shanghai, China; ST795) for 20 min to permeabilize and blocked with 5% bovine serum albumin (BSA; Beyotime Biotechnology Co., Ltd., Shanghai, China; ST023) for 1 h, followed by overnight exposure to primary antibodies targeting Aβ (Abcam, Cambridge, UK; ab201060), p-Tau-S396 (Abcam, Cambridge, UK; ab32057), p-Tau-Thr231 (Abcam, Cambridge, UK; ab151559). Following PBS washes, sections were exposed to appropriate species-specific Alexa Fluor–tagged secondary antibodies (anti-rabbit or anti-mouse IgG; Invitrogen, Carlsbad, CA, USA; A-11008 or A-11005) at room temperature for 1 h. DAPI (Beyotime Biotechnology Co., Ltd., Shanghai, China; C1005) was applied as a nuclear counterstain for 5 min, and samples were coverslipped with an antifade reagent (Beyotime Biotechnology Co., Ltd., Shanghai, China; P0126). Coronal brain sections containing the hippocampus were selected according to a standard mouse brain atlas, and fluorescence images were acquired from comparable hippocampal regions across all groups using laser confocal microscopy (Zeiss LSM 800, Carl Zeiss, Oberkochen, Germany). Mean fluorescence intensity was analyzed using ImageJ software (version 1.53, National Institutes of Health, Bethesda, MD, USA) to evaluate Aβ accumulation and Tau phosphorylation.

Western Blotting

Hippocampal tissues were homogenized in RIPA buffer (Guangzhou Yujia Biotechnology Co., Ltd., Guangzhou, China; L00399) to extract total protein, and the concentration was assessed using bicinchoninic acid (BCA) assay. For Western blotting, proteins (30 µg/lane) were separated by SDS-PAGE and transferred onto PVDF membranes (Millipore, USA, IPVH00010). Following a 1-h block with 5% skim milk at room temperature, membranes were treated overnight at 4 °C with primary antibodies targeting BACE1 (Abcam, Cambridge, UK; ab183612), Clathrin (Abcam, Cambridge, UK; ab21679), Nicastrin (Abcam, Cambridge, UK; ab3444), Iba1 (Abcam, Cambridge, UK; ab178846), GFAP (Abcam, Cambridge, UK; ab7260), Tau (Abcam, Cambridge, UK; ab92676), Tau (Ser396) (Abcam, Cambridge, UK; ab32057), NF-κB p65 subunit (p65, Abcam, Cambridge, UK; ab32536), inhibitor of nuclear factor kappa B alpha (IκBα, Abcam, Cambridge, UK; ab32518), p-IκBα (Abcam, Cambridge, UK; ab133462). Following primary antibody binding, membranes were treated with appropriate HRP-linked secondary antibodies (goat anti-rabbit or anti-mouse IgG; Cell Signaling Technology, Danvers, MA, USA; 7074 or 7076) at room temperature for 1 h. Protein bands were visualized with an enhanced chemiluminescence (ECL) detection reagent (Thermo Fisher Scientific, Waltham, MA, USA; 32106) and imaged by a chemiluminescence imaging system (Bio-Rad ChemiDoc XRS+, Hercules, CA, USA). Band intensities were quantified using ImageJ software (version 1.53, National Institutes of Health, Bethesda, MD, USA), and protein expression levels were normalized to β-actin.

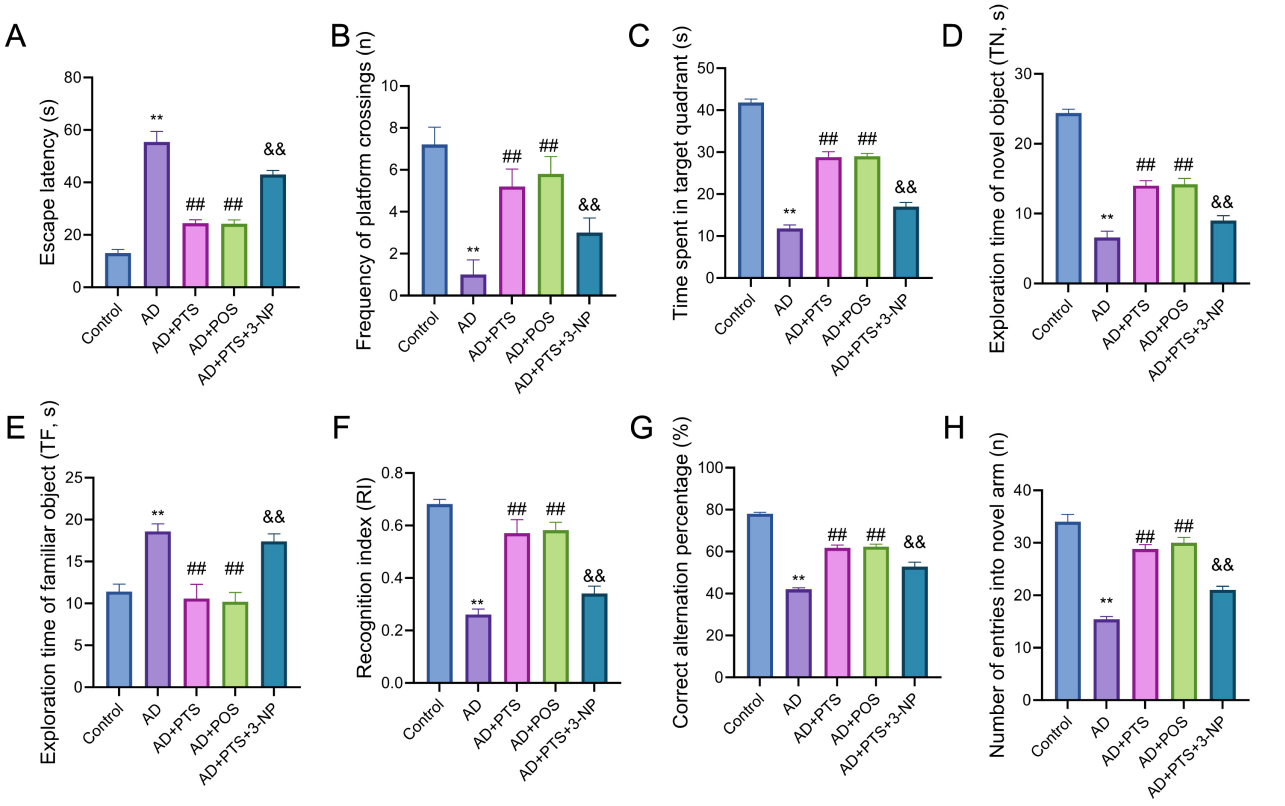

Fig. 1. Pterostilbene improves learning and memory impairments in AD mice. The Morris water maze (A–C), novel object recognition test (D–F), and Y-maze (G,H) were used to assess cognitive function in each group. (A) Escape latency (s); (B) Frequency of platform crossings (n); (C) Time spent in the target quadrant (s); (D) Exploration time of the novel object (TN, s); (E) Exploration time of familiar object (TF, s); (F) Recognition index (RI); (G) Correct alternation percentage (%); (H) Number of entries into the novel arm (n). $^{**}p < 0.01$ vs. Control; $^{\#\#}p < 0.01$ vs. AD; $^{\&\&}p < 0.01$ vs. AD+PTS. Data are presented as mean ± SD (n = 10 mice per group). AD, Alzheimer's disease; PTS, Pterostilbene; POS, positive control (donepezil); 3-NP, 3-nitropropionic acid; SD, standard deviation.

Table 1. Primer sequences utilized in the present study.

	Forward primer (5′-3′)	Reverse primer (5′-3′)	
Bace1	CCGTCATCATGGAAGGTTTC	ATGGCCGCCATGACATAGG	NM_001145947.3
Gapdh	AGGTCGGTGTGAACGGATTTG	TGTAGACCATGTAGTTGAGGTCA	NM_001289726.2

Reverse Transcription Quantitative Polymerase Chain Reaction (RT-qPCR)

RNA extraction was conducted using TRIzol reagent (Beyotime Biotechnology Co., Ltd., Shanghai, China; R0016). RNA concentration and purity were detected by a UV spectrophotometer (ThermoFisher Scientific, Waltham, MA, USA; 840-317400), and reverse transcription was performed to synthesize cDNA using a commercial kit (ThermoFisher Scientific, Waltham, MA, USA; SO131). qRT-PCR amplification was conducted with a SYBR Green kit (Guangzhou Yujia Biotechnology Co., Ltd., Guangzhou, China; D7268S). The amplification process began with an initial denaturation (95 °C, 10 min), then underwent forty amplification cycles (95 °C, 30 s; 60 °C, 30 s; 72 °C, 30 s). *Gapdh* (Mus musculus) was utilized as the reference gene, and mRNA expression was quantified via the $2^{-\Delta\Delta Ct}$ method. The primer sequences used for RT-qPCR are shown in Table 1. All reactions were conducted in triplicate.

Statistical Analysis

Statistical analyses were conducted with GraphPad Prism 8.0.2 (GraphPad Software, San Diego, CA, USA), and values are expressed as mean ± standard deviation (SD). Between-group differences were evaluated using one-way analysis of variance (ANOVA) followed by Tukey's post hoc test. For all analyses, n represents the number of mice in each group, and values obtained from multiple sections or fields were averaged per mouse before statistical analysis. Statistical significance was determined at $p < 0.05$.

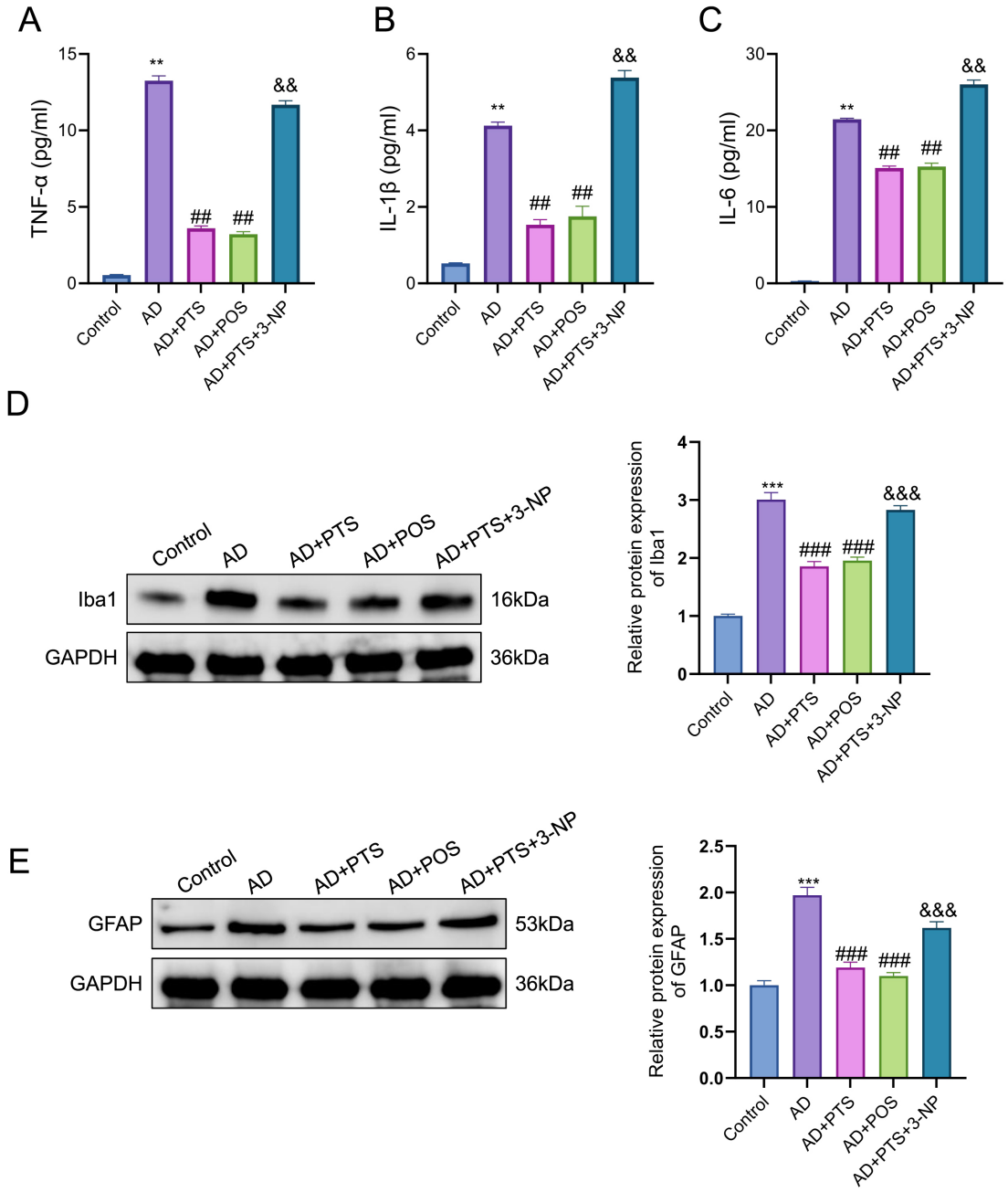

Fig. 2. Pterostilbene attenuates neuroinflammation in AD mice. (A–C) Inflammatory cytokine concentrations, including TNF-α (A), IL-1β (B), and IL-6 (C), were quantified using ELISA in hippocampal tissue homogenates of each group of mice. (D,E) Western blot analysis and corresponding quantitative results showing protein expression levels of Iba1 (D) and GFAP (E) in hippocampal tissues. $^{**}p < 0.01$, $^{***}p < 0.001$ vs. Control; $^{\#\#}p < 0.01$, $^{\#\#\#}p < 0.001$ vs. AD; $^{\&\&}p < 0.01$, $^{\&\&\&}p < 0.001$ vs. AD+PTS. Data are presented as mean ± SD (n = 10 mice per group). TNF-α, tumor necrosis factor-alpha; IL-1β, interleukin-1 beta; IL-6, interleukin-6; ELISA, Enzyme-linked immunosorbent assay; Iba1, ionized calcium-binding adaptor molecule 1; GFAP, glial fibrillary acidic protein.

Results

Pterostilbene Improves the Cognitive Function of AD Mice

In the Morris water maze test (Fig. 1A–C), AD mice exhibited longer escape latencies, fewer platform crossings, and less time spent in the target quadrant compared with controls ($p < 0.01$). Administration of PTS and POS significantly ameliorated these deficits ($p < 0.01$ vs. AD), whereas co-treatment with 3-nitropropionic acid (AD+PTS+3-NP) partially attenuated the effects of PTS ($p < 0.01$ vs. AD+PTS). In the novel object recognition test,

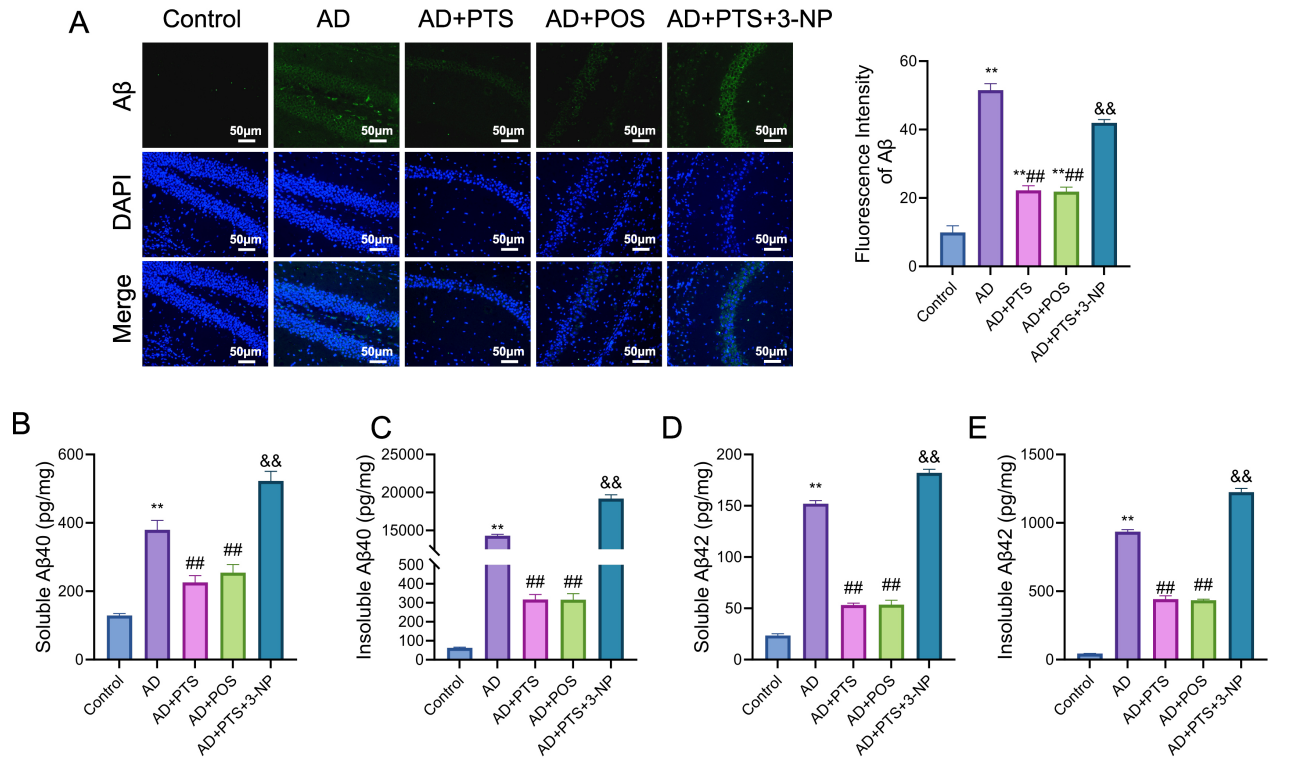

Fig. 3. Pterostilbene reduces hippocampal Aβ immunoreactive accumulation in AD mice. (A) Immunofluorescence micrographs illustrating Aβ immunoreactive deposits in the hippocampus, with quantitative analysis of Aβ fluorescence intensity shown on the right. (B–E) ELISA detecting the concentrations of soluble Aβ40 (B), insoluble Aβ40 (C), soluble Aβ42 (D), and insoluble Aβ42 (E) levels in brain tissue. $^{**}p < 0.01$ vs. Control; $^{\#\#}p < 0.01$ vs. AD; $^{\&\&}p < 0.01$ vs. AD+PTS. Data are presented as mean $\pm$ SD (n = 10 mice per group). Aβ, amyloid-β.

AD mice exhibited shortened exploration time of the novel object (Fig. 1D), prolonged exploration time of the familiar object (Fig. 1E), and reduced recognition index (Fig. 1F) ($p < 0.01$ vs. Control). PTS and POS interventions improved these parameters ($p < 0.01$ vs. AD), but AD+PTS+3-NP weakened the effect ($p < 0.01$ vs. AD+PTS). In the Y-maze test, AD mice showed a lower correct alternation percentage (Fig. 1G) and a reduced number of entries into the novel arm (Fig. 1H) ($p < 0.01$ vs. Control). These impairments were ameliorated by PTS and POS ($p < 0.01$ vs. AD), with reduced efficacy in the AD+PTS+3-NP group ($p < 0.01$ vs. AD+PTS). Overall, the above findings indicate that PTS improves learning, recognition memory, and spatial working memory in AD mice, and that these beneficial effects are partially attenuated by co-treatment with 3-NP.

Pterostilbene Reduces Neuroinflammation in AD Mice

To investigate the anti-inflammatory effects of PTS, inflammatory cytokine levels and glial activation–related protein expression were assessed in hippocampal tissues. TNF-α, IL-1β, and IL-6 levels were markedly elevated in the AD group relative to controls ($p < 0.01$) (Fig. 2A–C). Treatment with PTS and POS markedly reduced these pro-inflammatory cytokines ($p < 0.01$ vs. AD), whereas co-treatment with 3-nitropropionic acid (AD+PTS+3-NP) partially attenuated the anti-inflammatory effects of PTS ($p < 0.01$ vs. AD+PTS). Western blot analysis further demonstrated that protein expression levels of Iba1 (Fig. 2D) and GFAP (Fig. 2E) were significantly increased in the hippocampus of AD mice compared with controls ($p < 0.001$), indicating enhanced microglial and astrocytic activation at the protein level. Both PTS and POS treatments markedly reduced Iba1 and GFAP expression ($p < 0.001$ vs. AD), whereas the inhibitory effects were partially weakened in the AD+PTS+3-NP group ($p < 0.001$ vs. AD+PTS). Taken together, these findings indicate that PTS alleviates neuroinflammatory responses in AD mice, as evidenced by reduced pro-inflammatory cytokine production and downregulation of glial activation–associated proteins, effects that were partially weakened by co-treatment with 3-NP.

Pterostilbene Reduces Aβ Deposition in AD Mice

To determine whether PTS affects Aβ pathology, Aβ deposition and its soluble and insoluble forms were assessed. Immunofluorescence analysis showed that Aβ im-

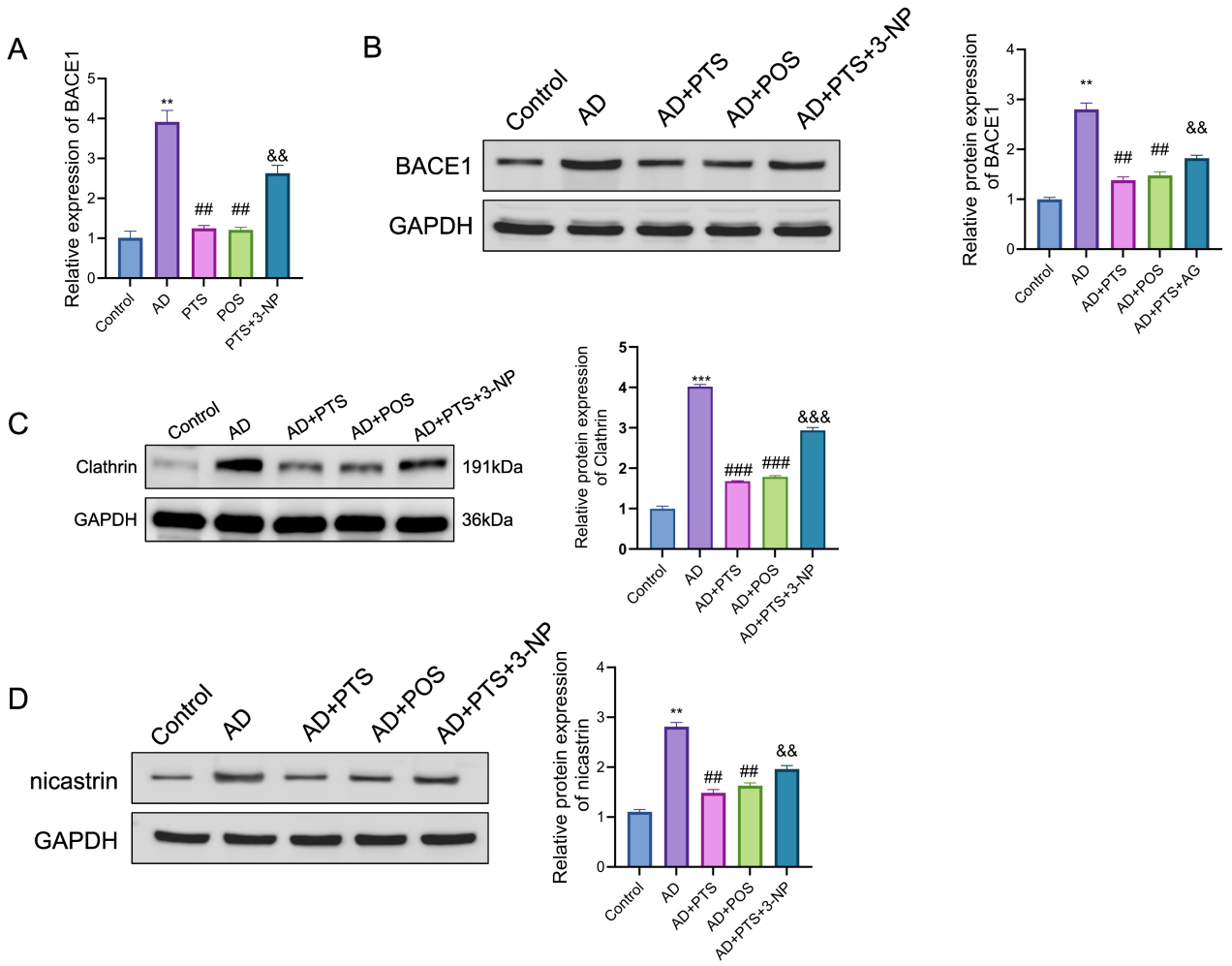

Fig. 4. Pterostilbene downregulates BACE1, Clathrin, and Nicastrin expression in AD mice. (A) Relative mRNA expression of BACE1 in hippocampal tissue quantified by RT-qPCR. (B–D) Western blotting and semi-quantitative evaluation of BACE1 (B), Clathrin (C), and Nicastrin (D) protein expression levels in each group. $^{**}p < 0.01$, $^{***}p < 0.001$ vs. Control; $^{\#\#}p < 0.01$, $^{\#\#\#}p < 0.001$ vs. AD; $^{\&\&}p < 0.01$, $^{\&\&\&}p < 0.001$ vs. AD+PTS. Data are presented as mean ± SD (n = 10 mice per group). BACE1, β-site amyloid precursor protein–cleaving enzyme 1; RT-qPCR, reverse transcription quantitative polymerase chain reaction.

munoreactive deposits in the hippocampus were substantially higher in AD mice than in controls ($p < 0.01$). PTS and POS treatments markedly reduced Aβ deposition ($p < 0.01$ vs. AD), while the AD+PTS+3-NP group exhibited higher Aβ levels relative to the PTS group ($p < 0.01$) (Fig. 3A). Consistently, ELISA results demonstrated elevated levels of soluble Aβ40 (Fig. 3B), insoluble Aβ40 (Fig. 3C), soluble Aβ42 (Fig. 3D), and insoluble Aβ42 (Fig. 3E) in the AD group ($p < 0.01$ vs. Control). PTS and POS significantly decreased both soluble and insoluble Aβ40 and Aβ42 levels ($p < 0.01$ vs. AD), whereas co-treatment with 3-NP increased these levels compared to PTS alone ($p < 0.01$). These results indicate that PTS reduces Aβ accumulation in AD mice, and that its beneficial effects are partially weakened by co-treatment with 3-NP.

Pterostilbene Inhibits BACE1 and Aβ Generation-Related Proteins

To deepen mechanistic insight into the effect of PTS on Aβ accumulation, BACE1 expression and Aβ production-related proteins, Clathrin and Nicastrin, were evaluated in hippocampal tissue. Both RT-qPCR and Western blot assays showed that BACE1 expression was notably upregulated in AD mice relative to controls ($p < 0.01$), whereas PTS and POS treatments markedly reduced BACE1 expression ($p < 0.01$ vs. AD). Co-treatment with 3-NP resulted in higher BACE1 expression than PTS alone ($p < 0.01$) (Fig. 4A,B). To supplement these findings, the basal hippocampal distribution of BACE1 in Control mice is shown in **Supplementary Fig. 1**. Notably, PTS did not alter BACE1 expression in Control mice (**Supplementary Fig. 2**), indicating that its effect is preferentially observed under pathological conditions.

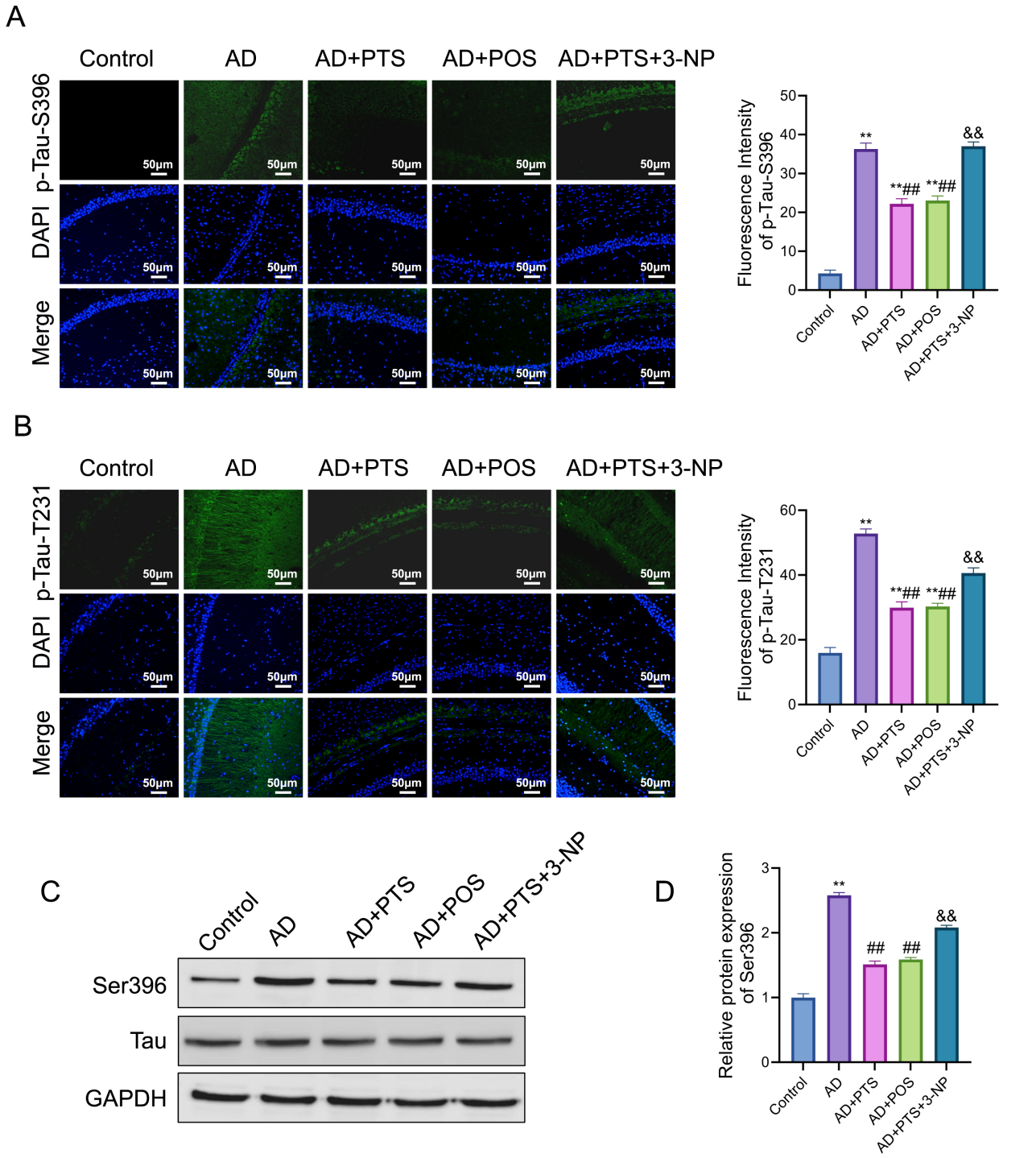

Fig. 5. Pterostilbene attenuates Tau phosphorylation in the hippocampus of AD mice. (A,B) Representative immunofluorescence micrographs and quantitative analysis of phosphorylated Tau at Ser396 (A) and Thr231 (B) in the hippocampus. (C,D) Western blotting (C) and semi-quantitative analysis (D) of p-Tau (Ser396) expression; total Tau and GAPDH served as controls. $^{**}p < 0.01$ vs. Control; $^{\#\#}p < 0.01$ vs. AD; $^{\&\&}p < 0.01$ vs. AD+PTS. Data are presented as mean ± SD (n = 10 mice per group). Tau, microtubule-associated protein tau.

In addition, Clathrin (Fig. 4C) and Nicastrin (Fig. 4D) protein levels were markedly elevated in the AD group ($p < 0.01$ vs. Control). PTS and POS treatments significantly decreased Clathrin and Nicastrin expression ($p < 0.01$ vs. AD), while the AD+PTS+3-NP group showed elevated levels compared to PTS treatment alone ($p < 0.01$).

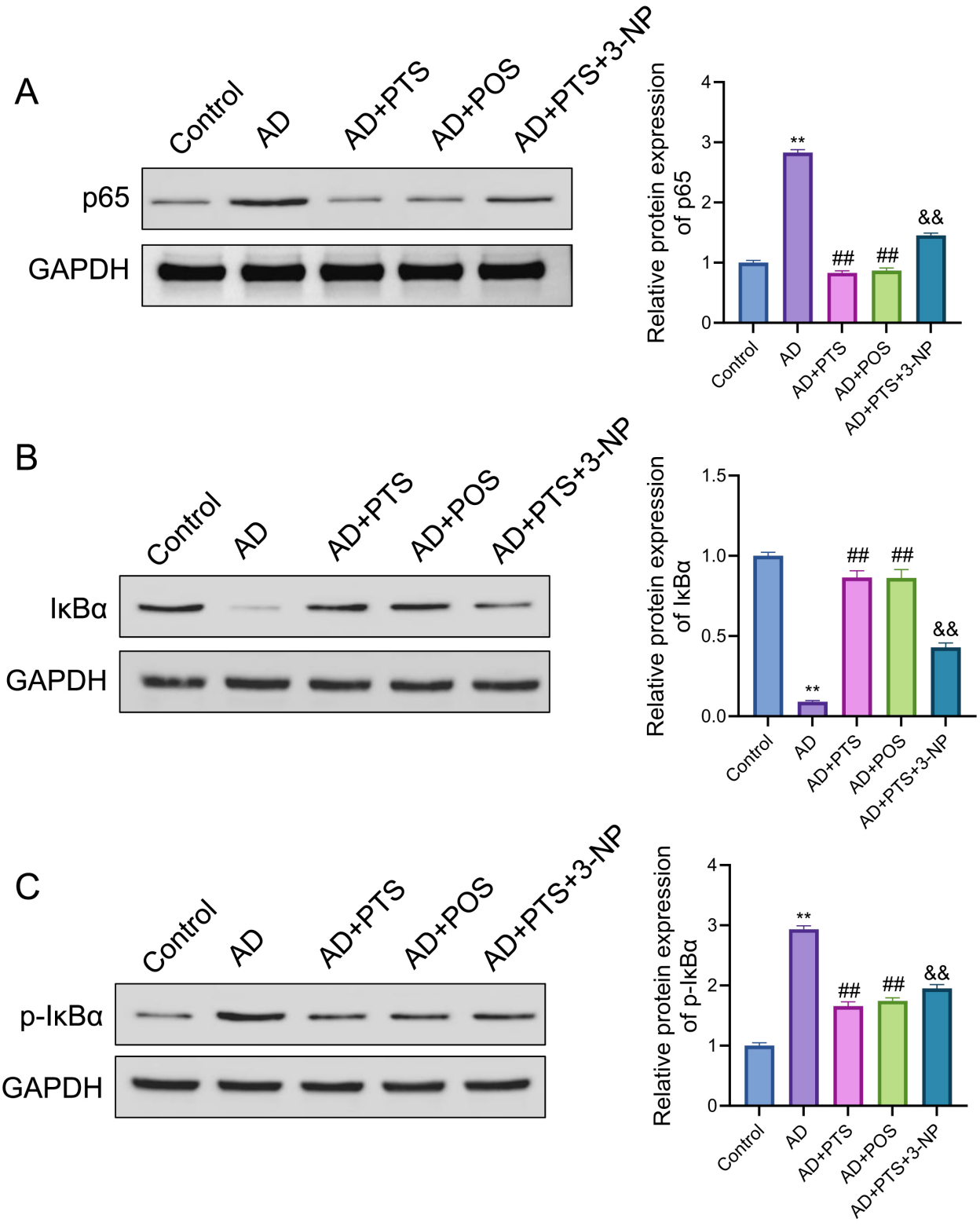

Fig. 6. Pterostilbene modulates NF-κB signaling in AD mice. (A–C) Western blot and semi-quantitative analyses of p65 (A), IκBα (B), and p-IκBα (C) protein levels in brain tissues. $^{**}p < 0.01$ vs. Control; $^{\#\#}p < 0.01$ vs. AD; $^{\&\&}p < 0.01$ vs. AD+PTS. Data are presented as mean ± SD (n = 10 mice per group). NF-κB, nuclear factor kappa B; IκBα, inhibitor of nuclear factor kappa B alpha; p-IκBα, phosphorylated IκBα.

These results show that PTS is related to reduced expression of BACE1 and Aβ generation–related proteins in AD mice, and that these effects are partially attenuated by co-treatment with 3-nitropropionic acid.

Pterostilbene Inhibits Abnormal Phosphorylation of Tau Protein in AD Mice

To determine whether PTS inhibits Tau protein hyperphosphorylation, the expression of p-Tau at Ser396 and Thr231 was evaluated. Immunofluorescence analysis showed that p-Tau (Ser396) (Fig. 5A) and p-Tau (Thr231) (Fig. 5B) levels were significantly increased in the hippocampus of AD mice compared with controls ($p < 0.01$). Both PTS and POS treatments markedly reduced p-Tau expression ($p < 0.01$ vs. AD), whereas co-treatment with 3-NP partially attenuated the inhibitory effects of PTS ($p < 0.01$ vs. AD+PTS). Consistently, Western blot analysis confirmed that p-Tau (Ser396) expression was markedly elevated in AD mice ($p < 0.01$ vs. Control), but significantly decreased following PTS and POS treatment ($p < 0.01$ vs. AD). In contrast, p-Tau (Ser396) levels in the AD+PTS+3-NP group were significantly elevated compared to the PTS group ($p < 0.01$) (Fig. 5C,D). These results show that PTS is associated with reduced Tau hyperphosphorylation in AD mice, an effect that is partially weakened by co-treatment with 3-NP.

Pterostilbene Modulates the NF-κB Signaling in AD Mice

To examine the effects of PTS on NF-κB signaling, brain tissue expression of p65, IκBα, and p-IκBα was assessed via Western blotting. AD mice exhibited significantly increased p65 and p-IκBα levels accompanied by reduced IκBα expression compared with controls ($p < 0.01$), indicating enhanced NF-κB pathway activation. PTS and POS treatments markedly reversed these alterations, as reflected by decreased p65 and p-IκBα levels and elevated IκBα expression ($p < 0.01$ vs. AD). In contrast, co-treatment with 3-nitropropionic acid (AD+PTS+3-NP) partially diminished PTS's inhibitory effects on NF-κB signaling cascade ($p < 0.01$ vs. AD+PTS) (Fig. 6A–C). Collectively, these findings demonstrate that PTS is linked to suppression of NF-κB pathway activation in AD mice, an effect that is partially weakened by co-treatment with 3-NP.

Discussion

This study demonstrates that PTS markedly improves cognitive function and ameliorates multiple pathological features in an Aβ1-42–induced AD mouse model. Specifically, PTS enhanced spatial learning, memory, and object recognition, reduced neuroinflammation (as reflected by decreased pro-inflammatory cytokine levels and decreased expression of microglia- and astrocyte-associated proteins), decreased hippocampal Aβ immunoreactive accumulation and Aβ40/Aβ42 levels, and reduced Tau protein phosphorylation accompanied by modulation of NF-κB signaling. Notably, co-treatment with 3-nitropropionic acid partially attenuated the protective effects of PTS across behavioral, inflammatory, and molecular outcomes. Together, these results indicate that PTS exerts broad neuroprotective functions via coordinated regulation of multiple pathological processes relevant to AD, while implicating the involvement of BACE1-associated and inflammation-related signaling pathways in mediating its efficacy.

It should be noted that intraperitoneal administration of aggregated Aβ1-42 was not intended to model classical amyloid plaque seeding via direct blood–brain barrier penetration, but rather to induce Aβ-associated neuroinflammatory responses and secondary amyloidogenic alterations in the brain. Peripheral pathological stimuli, including systemic inflammation or peripheral Aβ exposure, have been shown to promote endogenous amyloidogenic processes through inflammatory signaling and blood–brain barrier dysfunction [25,26]. Accordingly, the hippocampal Aβ immunoreactive deposits observed in this study likely reflect neuroinflammation-driven secondary amyloid accumulation rather than direct deposition of exogenous Aβ, and all mechanistic interpretations, including changes in BACE1 expression, are made within the context of this model.

The neuroprotective effects of PTS observed in the present study are consistent with previous reports. Accumulating evidence indicates that PTS ameliorates pathological features of neurodegenerative diseases through anti-inflammatory and antioxidant mechanisms. For example, in Parkinson's disease models, PTS has been shown to attenuate inflammation and oxidative stress [27], while in AD models, PTS reduces Aβ deposition and improves cognitive performance [28]. Consistent with these findings, our results demonstrate that PTS significantly suppresses neuroinflammatory responses in AD mice, as evidenced by reduced levels of pro-inflammatory cytokines (TNF-α, IL-1β, and IL-6) together with downregulation of microglia- and astrocyte-associated protein expression, thereby alleviating inflammation-associated AD pathology. Moreover, PTS treatment markedly decreased hippocampal Aβ40 and Aβ42 levels as well as Aβ immunoreactive deposition, further supporting its role in mitigating Aβ pathology. Beyond corroborating existing studies, the present study offers mechanistic insights into the function of NF-κB signaling in PTS-mediated neuroprotection. While the pivotal function of NF-κB signaling in neuroinflammation has been well documented [29,30], its contribution to the regulation of Aβ accumulation and Tau phosphorylation in the context of PTS treatment has remained unclear. Our data show that PTS markedly suppresses NF-κB pathway overactivation by inhibiting p65 nuclear translocation and reducing p-IκBα levels, while restoring IκBα expression. These molecular changes may account for the dual effects

of PTS on attenuating neuroinflammation and reducing abnormal Tau phosphorylation. Notably, this study systematically evaluates the impact of PTS on Tau phosphorylation at Ser396 and Thr231, providing further evidence that PTS exerts multi-target neuroprotective actions through modulation of NF-κB–related pathological processes.

In addition to its well-documented role in Aβ production, *Bace1* has also been linked to the modulation of neuroinflammatory responses and Tau phosphorylation through downstream signaling pathways. Earlier investigations have demonstrated that increased *Bace1* activity contributes to Aβ accumulation, thereby exacerbating neuroinflammation and promoting Tau pathology, which collectively drive AD progression [31,32]. Although pharmacological inhibition of BACE1 has demonstrated efficacy in reducing Aβ levels, clinical trials have yielded limited success, partly due to off-target effects and an incomplete understanding of downstream consequences [33]. In the present study, PTS treatment was associated with reduced *Bace1* expression, accompanied by decreased Aβ deposition, attenuated neuroinflammatory responses, and suppression of Tau phosphorylation, thereby extending current evidence linking *Bace1* to multiple pathological processes in AD. Notably, 3-NP treatment partially attenuated the neuroprotective effects of PTS, consistent with a role for BACE1-related pathways in regulating these responses. Importantly, PTS did not alter basal BACE1 levels in Control mice but selectively reduced pathological BACE1 upregulation in AD mice. Collectively, these findings suggest that modulation of *Bace1*-associated processes by natural compounds such as PTS may represent a multi-target therapeutic strategy with potentially fewer adverse effects than direct BACE1 inhibition, providing additional insight into optimizing AD treatment approaches.

The multi-target mechanism of action of PTS provides a new perspective for AD treatment. This study combined behavioral, ELISA, immunofluorescence, Western blot and other experimental approaches to systematically evaluate the intervention effect of PTS in AD. It not only verified the role of PTS in mitigating neuroinflammation and Aβ pathology, but also provides mechanistic insights into the involvement of the NF-κB signaling pathway in linking neuroinflammation to Tau phosphorylation during AD progression. These results provide important theoretical support for advancing multi-target therapeutic approaches derived from natural compounds, and also lay a rational basis for the promising clinical utility of PTS in AD therapy.

Although the present study provides evidence supporting the neuroprotective properties of PTS in an Aβ1-42-induced AD mouse model, several limitations should be noted. First, this model primarily reflects inflammation-associated amyloidogenic alterations rather than classical plaque-seeding pathology, and the effects of PTS were not validated in other AD models, such as transgenic mice, which may restrict the broader application of the findings. Second, 3-nitropropionic acid was used as a pharmacological perturbation associated with BACE1 upregulation; however, given its known off-target effects and the absence of a 3-NP-only control group or systematic toxicity assessment, conclusions regarding BACE1-related signaling are based on associative rather than causal evidence. In addition, the long-term safety and dose–response profile of PTS were not comprehensively evaluated. Future studies employing multiple AD models, more specific mechanistic approaches, and comprehensive safety assessments are warranted to further clarify the multi-target actions of PTS.

Conclusion

This study demonstrates that PTS significantly ameliorates pathological features in AD mice, as evidenced by improved cognitive performance, decreased neuroinflammation, reduced Aβ accumulation, and inhibition of abnormal Tau phosphorylation. These effects are associated with modulation of the NF-κB signaling pathway, suggesting a multi-target mechanism of action. Collectively, these findings highlight the therapeutic potential of PTS as a natural compound for Alzheimer's disease and provide a theoretical basis for developing multi-target treatment strategies.

Availability of Data and Materials

The data used to support the findings of this study are available from the corresponding author upon request.

Author Contributions

XMW and MTZ contributed to conception and design; XMW, LYL and MTZ made substantial contributions to acquisition of data; HTL and XMW analyzed and interpreted data; XMW was involved in drafting the manuscript; HTL, LYL and MTZ were involved in revising it critically for important intellectual content. All authors gave final approval of the version to be published and agreed to be accountable for all aspects of the work.

Ethics Approval and Consent to Participate

All experimental procedures involving animals complied with the institutional guidelines and were approved by the Experimental Animal Welfare Ethics Committee of Capital Medical University (Protocol No. AEEI-2020-139).

Acknowledgment

Not applicable.

Funding

This study is supported by Capital Medical University Scientific Research Innovation Project (XSKY2022435, XSKY2023192).

Conflict of Interest

The authors declare no conflict of interest.

Supplementary Material

Supplementary material associated with this article can be found, in the online version, at https://doi.org/10.24976/Discov.Med.202638206.65.

References

[1] Weller J, Budson A. Current understanding of Alzheimer's disease diagnosis and treatment. F1000Research. 2018; 7: F1000 Faculty Rev–1161. https://doi.org/10.12688/f1000research.14506.1.

[2] Jack CR, Jr, Bennett DA, Blennow K, Carrillo MC, Dunn B, Haeberlein SB, *et al*. NIA-AA Research Framework: Toward a biological definition of Alzheimer's disease. Alzheimer's & Dementia: the Journal of the Alzheimer's Association. 2018; 14: 535–562. https://doi.org/10.1016/j.jalz.2018.02.018.

[3] Zhang XX, Tian Y, Wang ZT, Ma YH, Tan L, Yu JT. The Epidemiology of Alzheimer's Disease Modifiable Ri Alzheimer's Disease sk Factors and Prevention. The Journal of Prevention of Alzheimer's Disease. 2021; 8: 313–321. https://doi.org/10.14283/jpad.2021.15.

[4] GBD 2019 Dementia Forecasting Collaborators. Estimation of the global prevalence of dementia in 2019 and forecasted prevalence in 2050: an analysis for the Global Burden of Disease Study 2019. The Lancet. Public Health. 2022; 7: e105–e125. https://doi.org/10.1016/S2468-2667(21)00249-8.

[5] Wang H, Qin D, Fang L, Liu H, Song P. Addressing healthy aging in China: Practices and prospects. Bioscience Trends. 2024; 18: 212–218. https://doi.org/10.5582/bst.2024.01180.

[6] Srivastava S, Ahmad R, Khare SK. Alzheimer's disease and its treatment by different approaches: A review. European Journal of Medicinal Chemistry. 2021; 216: 113320. https://doi.org/10.1016/j.ejmech.2021.113320.

[7] Cummings J, Lee G, Nahed P, Kambar MEZN, Zhong K, Fonseca J, *et al*. Alzheimer's disease drug development pipeline: 2022. Alzheimer's & Dementia (New York, N. Y.). 2022; 8: e12295. https://doi.org/10.1002/trc2.12295.

[8] Cummings JL, Tong G, Ballard C. Treatment Combinations for Alzheimer's Disease: Current and Future Pharmacotherapy Options. Journal of Alzheimer's Disease: JAD. 2019; 67: 779–794. https://doi.org/10.3233/JAD-180766.

[9] Guo J, Wang Z, Liu R, Huang Y, Zhang N, Zhang R. Memantine, Donepezil, or Combination Therapy-What is the best therapy for Alzheimer's Disease? A Network Meta-Analysis. Brain and Behavior. 2020; 10: e01831. https://doi.org/10.1002/brb3.1831.

[10] Liu W, Li Y, Zhao T, Gong M, Wang X, Zhang Y, *et al*. The role of N-methyl-D-aspartate glutamate receptors in Alzheimer's disease: From pathophysiology to therapeutic approaches. Progress in Neurobiology. 2023; 231: 102534. https://doi.org/10.1016/j.pneurobio.2023.102534.

[11] Pandey MK. Complement Inhibition Expands the Therapeutic Window of Amyloid-β Immunotherapy in Alzheimer's Disease. Discovery Medicine. 2025, 37: 1409–1415. https://doi.org/10.24976/Discov.Med.202537198.122.

[12] Kalra J, Khan A. Reducing Aβ load and tau phosphorylation: Emerging perspective for treating Alzheimer's disease. European Journal of Pharmacology. 2015; 764: 571–581. https://doi.org/10.1016/j.ejphar.2015.07.043.

[13] Gong CX, Grundke-Iqbal I, Iqbal K. Targeting tau protein in Alzheimer's disease. Drugs & Aging. 2010; 27: 351–365. https://doi.org/10.2165/11536110-000000000-00000.

[14] Zhou DD, Cheng J, Li J, Wu SX, Xiong RG, Huang SY, *et al*. Resveratrol and Its Analogues: Anti-ageing Effects and Underlying Mechanisms. Sub-cellular Biochemistry. 2024; 107: 183–203. https://doi.org/10.1007/978-3-031-66768-8_9.

[15] Shen B, Wang Y, Cheng J, Peng Y, Zhang Q, Li Z, *et al*. Pterostilbene alleviated NAFLD via AMPK/mTOR signaling pathways and autophagy by promoting Nrf2. Phytomedicine: International Journal of Phytotherapy and Phytopharmacology. 2023; 109: 154561. https://doi.org/10.1016/j.phymed.2022.154561.

[16] Abd-Elmawla MA, Abdelalim E, Ahmed KA, Rizk SM. The neuroprotective effect of pterostilbene on oxaliplatin-induced peripheral neuropathy via its anti-inflammatory, anti-oxidative and anti-apoptotic effects: Comparative study with celecoxib. Life Sciences. 2023; 315: 121364. https://doi.org/10.1016/j.lfs.2022.121364.

[17] Nagumo M, Ninomiya M, Oshima N, Itoh T, Tanaka K, Nishina A, *et al*. Comparative analysis of stilbene and benzofuran neolignan derivatives as acetylcholinesterase inhibitors with neuroprotective and anti-inflammatory activities. Bioorganic & Medicinal Chemistry Letters. 2019; 29: 2475–2479. https://doi.org/10.1016/j.bmcl.2019.07.026.

[18] Li Q, Li X, Tian B, Chen L. Protective effect of pterostilbene in a streptozotocin-induced mouse model of Alzheimer's disease by targeting monoamine oxidase B. Journal of Applied Toxicology: JAT. 2022; 42: 1777–1786. https://doi.org/10.1002/jat.4355.

[19] Chang J, Rimando A, Pallas M, Camins A, Porquet D, Reeves J, *et al*. Low-dose pterostilbene, but not resveratrol, is a potent neuromodulator in aging and Alzheimer's disease. Neurobiology of Aging. 2012; 33: 2062–2071. https://doi.org/10.1016/j.neurobiolaging.2011.08.015.

[20] Zhou J, Singh N, Galske J, Hudobenko J, Hu X, Yan R. BACE1 regulates expression of Clusterin in astrocytes for enhancing clearance of β-amyloid peptides. Molecular Neurodegeneration. 2023; 18: 31. https://doi.org/10.1186/s13024-023-00611-w.

[21] Wang YR, Zeng XQ, Wang J, Fowler CJ, Li QX, Bu XL, *et al*. Autoantibodies to BACE1 promote Aβ accumulation and neurodegeneration in Alzheimer's disease. Acta Neuropathologica. 2024; 148: 57. https://doi.org/10.1007/s00401-024-02814-x.

[22] Stine WB, Jr, Dahlgren KN, Krafft GA, LaDu MJ. In vitro characterization of conditions for amyloid-beta peptide oligomerization and fibrillogenesis. The Journal of Biological Chemistry. 2003; 278: 11612–11622. https://doi.org/10.1074/jbc.M210207200.

[23] Lu L, Fu Z, Wu B, Zhang D, Wang Y. Leptin ameliorates Aβ1-42-induced Alzheimer's disease by suppressing inflammation via activating p-Akt signaling pathway. Translational Neuroscience. 2023; 14: 20220270. https://doi.org/10.1515/tnsci-2022-0270.

[24] Velliquette RA, O'Connor T, Vassar R. Energy inhibition elevates beta-secretase levels and activity and is potentially amyloidogenic in APP transgenic mice: possible early events in Alzheimer's disease pathogenesis. The Journal of Neuroscience: the Official Journal of the Society for Neuroscience. 2005; 25: 10874–10883. https://doi.org/10.1523/JNEUROSCI.2350-05.2005.

[25] Lai PH, Wang TH, Zhang NY, Wu KC, Yao CCJ, Lin CJ. Changes of blood-brain-barrier function and transfer of amyloid beta in rats with collagen-induced arthritis. Journal of Neuroinflammation. 2021; 18: 35. https://doi.org/10.1186/s12974-021-02086-2.

[26] Marottoli FM, Katsumata Y, Koster KP, Thomas R, Fardo DW, Tai LM. Peripheral Inflammation, Apolipoprotein E4, and Amyloid-β Interact to Induce Cognitive and Cerebrovascular Dysfunction. ASN Neuro. 2017; 9: 1759091417719201. https://doi.org/10.1177/1759091417719201.

[27] Fan Y, He X, Chen M, Guo S, Dong Z. Pterostilbene alleviates MPTP-induced neurotoxicity by targeting neuroinflammation and oxidative stress. Biochemical and Biophysical Research Communications. 2024; 729: 150358. https://doi.org/10.1016/j.bbrc.2024.150358.

[28] Xu J, Liu J, Li Q, Li G, Zhang G, Mi Y, *et al*. Pterostilbene participates in TLR4- mediated inflammatory response and autophagy-dependent Aβ_1 − 42 endocytosis in Alzheimer's disease. Phytomedicine: International Journal of Phytotherapy and Phytopharmacology. 2023; 119: 155011. https://doi.org/10.1016/j.phymed.2023.155011.

[29] Singh SS, Rai SN, Birla H, Zahra W, Rathore AS, Singh SP. NF-κB-Mediated Neuroinflammation in Parkinson's Disease and Potential Therapeutic Effect of Polyphenols. Neurotoxicity Research. 2020; 37: 491–507. https://doi.org/10.1007/s12640-019-00147-2.

[30] Wahl D, Risen SJ, Osburn SC, Emge T, Sharma S, Gilberto VS, *et al*. Nanoligomers targeting NF-κB and NLRP3 reduce neuroinflammation and improve cognitive function with aging and tauopathy. Journal of Neuroinflammation. 2024; 21: 182. https://doi.org/10.1186/s12974-024-03182-9.

[31] Barroso E, del Valle J, Porquet D, Vieira Santos AM, Salvadó L, Rodríguez-Rodríguez R, *et al*. Tau hyperphosphorylation and increased BACE1 and RAGE levels in the cortex of PPARβ/δ-null mice. Biochimica et Biophysica Acta. 2013; 1832: 1241–1248. https://doi.org/10.1016/j.bbadis.2013.03.006.

[32] Webers A, Heneka MT, Gleeson PA. The role of innate immune responses and neuroinflammation in amyloid accumulation and progression of Alzheimer's disease. Immunology and Cell Biology. 2020; 98: 28–41. https://doi.org/10.1111/imcb.12301.

[33] Millot P, San C, Bennana E, Porte B, Vignal N, Hugon J, *et al*. STAT3 inhibition protects against neuroinflammation and BACE1 upregulation induced by systemic inflammation. Immunology Letters. 2020; 228: 129–134. https://doi.org/10.1016/j.imlet.2020.10.004.